

AD A089193

DDC FILE COPY

SECURITY CLASSIFICATION OF THIS REPORT (When Data Entered)

REPORT DOCUMENTATION PAGE

READ INSTRUCTIONS BEFORE COMPLETING FORM

1. REPORT NUMBER Technical Report #11	2. GOVT ACCESSION NO. AD A089193	3. RECIPIENT'S ORG. USE NUMBER (14) TR-11
4. TITLE (and Subtitle) Fluid Transport into Crazes under Triaxial Stress.	4. DATE OF REPORT & PERIOD COVERED Technical Report Interim	
7. AUTHOR(s) Abdelsamie Moet and Eric Baer	5. CONTRACT OR GRANT NUMBER(s) N00014-75-C-0795	6. PERFORMING ORG. REPORT NUMBER
9. PERFORMING ORGANIZATION NAME AND ADDRESS Department of Macromolecular Science Case Western Reserve University Cleveland, Ohio 44106	10. PROGRAM ELEMENT, PROJECT, TASK AREA & WORK UNIT NUMBERS	
11. CONTROLLING OFFICE NAME AND ADDRESS Office of Naval Research (Code 472) Arlington, Virginia 22217	12. REPORT DATE August 25, 1980	13. NUMBER OF PAGES
14. MONITORING AGENCY NAME & ADDRESS (if different from Controlling Office) 12 33	15. SECURITY CLASS. (of this report) Unclassified	
16. DISTRIBUTION STATEMENT (of this Report) Approved for public release; distribution unlimited. Reproduction in whole or in part is permitted for any purpose of the United States Government.		
17. DISTRIBUTION STATEMENT (of the abstract entered in Block 20, if different from Report) DTIC ELECTE SEP 16 1980		
18. SUPPLEMENTARY NOTES A		
19. KEY WORDS (Continue on reverse side if necessary and identify by block number) Polystyrene, Crazes, Silicone oil, Penetration coefficient, Tension, Pressure, Maximum normal stress, Capillary pressure, Effective axial strain, Craze suppression		
20. ABSTRACT (Continue on reverse side if necessary and identify by block number) The penetration coefficient of silicone oil (500 cS) into PS during tensile deformation was determined under a range of superposed hydrostatic pressure of 1 to 1200 bars. At atmospheric pressure, the liquid front, driven by a relatively high capillary pressure, was found to lag behind the "dry" craze tip front. The penetrability was observed to increase as a steep linear function of the pressure up to 80 bars at which		

80 9 12 018  
SECURITY CLASSIFICATION OF THIS PAGE (When Data Entered)  
408357

the liquid front was forced to reach the craze tip front. At higher pressures, a stage of suppressed penetrability was observed which was associated with a substantial decrease in the craze size and density. The suppressed penetrability is explained on the basis of pressure-induced "void" reduction competing with its pumping component. An effective axial strain analysis is presented to explain such a reduction. The effect of pressure on the maximum stress at the tip of a flaw, in conjunction with the distribution of surface defects, is found to account for the suppressed craze density at elevated pressures.

CASE WESTERN RESERVE UNIVERSITY  
Department of Macromolecular Science  
Cleveland, Ohio 44106

Technical Report No. 11

FLUID TRANSPORT INTO CRAZES UNDER TRIAXIAL STRESS

BY

Abdelsamie Moet and Eric Baer  
Department of Macromolecular Science  
Case Western Reserve University  
Cleveland, Ohio 44106

August 25, 1980

Research Sponsored by the  
Office of Naval Research

Accession Number	
Date	
Author	
Title	
Institution	
Availability	
Notes	
Abstract	
Keywords	
Subject Terms	
Dissertation/Thesis	
Dist	
Special	

A

Contract N00014-75-C-0795

ABSTRACT

The penetration coefficient of silicone oil (500 cS) into PS during tensile deformation was determined under a range of superposed hydrostatic pressure of 1 to 1200 bars. At atmospheric pressure, the liquid front, driven by a relatively high capillary pressure, was found to lag behind the "dry" craze tip front. The penetrability was observed to increase as a steep linear function of the pressure up to 80 bars at which the liquid front was forced to reach the craze tip front. At higher pressures, a stage of suppressed penetrability was observed which was associated with a substantial decrease in the craze size and density. The suppressed penetrability is explained on the basis of pressure-induced "void" reduction competing with its pumping component. An effective axial strain analysis is presented to explain such a reduction. The effect of pressure on the maximum stress at the tip of a flaw, in conjunction with the distribution of surface defects, is found to account for the suppressed craze density at elevated pressures.

1. INTRODUCTION

In an earlier publication<sup>1</sup>, we reported on the mechanism of the pressure-induced environmental stress cracking in polystyrene (PS). Fourier Transform Infrared (FTIR) difference spectroscopy was used for the first time to measure small amounts of environmental fluid that penetrate the polymer during deformation. The penetrability of silicone oil into PS, estimated from a newly introduced penetration coefficient, was found to increase more than two orders of magnitude within the first 100 MPa above atmospheric pressure when a tensile load was exerted on the sample. The effect of pressure on the transport kinetics in this range has a special significance which may be illustrated by the two following points. The first is that the hydrostatic pressure under which a polymer may serve in an engineering application most probably would not exceed the 100 MPa limit. A second important point is that the discovery of a possible penetrability maximum in this pressure range due to a tensile load may offer extremely useful consequences in the preparation of high strength impregnated composites<sup>2,3</sup>.

Studies in this pressure regime may provide useful information to further resolve the controversy of transport behavior of liquids into crazes and its relation to craze growth and fracture.

Following the evidence presented earlier<sup>1</sup> for the "dry tip" craze growth, a situation which is not believed to prevail at high pressures, it would be useful to determine the pressure at which the fluid reaches the craze tip and the influence of such an event on the environmental stress cracking phenomenon. Other questions that remain to be answered include the nature of the driving force of liquids into crazes and the mechanism by which the pressure suppresses density and size of crazes.

This investigation studies primarily the transport behavior of silicone oil into polystyrene (crazes) under triaxial stress conditions with special emphasis on the pressure range 1 to 100 MPa. A relationship between the transport kinetics and craze growth will also be sought.

## 2. EXPERIMENTAL PROCEDURE

The experiments were conducted on commercial polystyrene using silicone oil as an environmental fluid. Material characteristics, sample geometry and methods of preparation are detailed in a previous publication<sup>1</sup>. In short, cylindrical specimens with an overall length of 6 cm. and reduced diameter of 0.3 cm. were exposed to a fixed elongation of 0.8% in silicone oil (500 cS) for an hour under varying superposed hydrostatic pressures. In another experiment designed to elucidate the nature of the force driving the liquid into crazes, samples were extensively crazed in air, for four hours at 1% fixed elongation, then placed in the oil for various periods of time. Additional unloaded soaking experiments have been performed on samples previously deformed in the environmental fluid and shall be described in the next section.

Tensile experiments under atmospheric pressure were conducted in an instron testing machine whereas high pressure testing was carried out in a Pugh-type high pressure apparatus<sup>4</sup> which is essentially a constant cross-head speed tensile machine contained within a pressure chamber filled with pressure-transmitting fluid (silicone oil). The desired hydrostatic pressure was applied, then the sample was deformed axially at about 10%/min to the predesigned elongation. The applied pressure and elongation were held constant throughout the span of the experiment.

Conventionally, the pressure is monitored by a manganin coil whose sensitivity is in the order of 0.1 kbar. However, because the study of the transport behavior in the range of 1 to 100 bars is a major objective of this investigation, a new pressure sensing mechanism capable of measuring much smaller pressures was designed.

A DC-DC differential pressure transducer (Wiancko P2-3000 series, C. J. Enterprise, California) was installed in the window plug of the pressure chamber. Prior to its installation, the transducer was calibrated using a dead weight gauge. A constant current input of 24.6 vDC was applied to the transducer and the output measured by a highly sensitive digital voltmeter ( $\pm 0.1$  mv) was translated into pressure from the calibration curve. This device has been applied only to measurements in the sub-100 bar range; above this range the conventional manganin coil method was used.

The radial concentration profile of silicone oil penetrant was measured by performing FTIR difference spectroscopy on successive layers milled along the gauge length of the sample. The penetration coefficient  $\kappa$  ( $\text{cm}^2/\text{sec}$ ) was evaluated from fitting the normalized concentration profiles to solutions of the expression derived earlier<sup>1</sup> to describe this penetration process.

In case of the unloaded soaking experiments, the concentration were directly expressed in terms of relative IR absorbance units of the Si-CH<sub>3</sub> methyl rocking vibration band at 1260 cm<sup>-1</sup>.

### 3. RESULTS AND DISCUSSION

#### 3.1. Transport Behavior

The transport behavior of silicone oil (500 cS) into PS has been determined by exerting a constant tensile strain of 0.8% on samples soaked in the oil for one hour. The penetration coefficient  $\kappa$  was estimated from fitting the concentration profiles into numerical solutions of the penetrability equation<sup>1</sup>

$$\frac{\partial C}{\partial t} = \frac{1}{r} \frac{\partial}{\partial r} (r \kappa \frac{\partial C}{\partial r})$$

where  $C$  is the fluid concentration at radius  $r$ , the diminishing radius of the dry core at time  $t$ . The magnitude of the fixed elongation was selected so that  $\kappa t / a^2$  at one hour is less than 1.

Figure 1 shows the relationship between the applied pressure and the one hour penetration coefficient expressed on a semi-logarithmic scale. In general, the transport behavior appears to fall into two distinct stages: a pressure-enhanced penetrability followed by a stage of pressure-suppressed transport. In the first stage, the penetrability increases dramatically as a linear function of the applied pressure. Within 800 bars,  $\kappa$  increases more than two orders of magnitude. In this stage, the number and size of crazes were noticed to increase with increasing pressure. Furthermore, FTIR measurements indicated that the depth of oil

penetration into the sample also increased as a function of pressure. The first stage ends in a maximum at about 80 bars.

In the pressure span from 80 to about 1200 bars, the penetration coefficient was observed to fall into two regimes. These two regimes have been observed in an earlier investigation<sup>1</sup>. In regime I, the rate of decrease in the penetration coefficient approximates seven times that observed in regime II. In both regimes I and II, the number and size of crazes were noticed to decrease dramatically with increasing pressure. Beyond regime II, only a few meager crazes were observed along the gauge length of the specimen without meaningful detection of any oil penetration. At pressures well above those in regime II, the polymer was observed to behave in a "super brittle" manner in which no crazes were observed for much longer exposure to silicone oil (and other liquids) under fixed elongations up to 1%.

### 3.2. Additional Unloaded Soaking

To determine the positional relationship between the craze "tip" front and the penetrant liquid front in the two stages described, unloaded soaking experiments were conducted. In one experiment, samples were elongated to 0.8% in silicone oil at 10 bars for one hour, after which the stress was released. Some of the samples were analyzed immediately for penetration while others were retained

in their liquid environment, unloaded, for additional soaking. Results of this experiment are shown in Fig. 2A. The oil front was found to advance deeper into the specimens soaked for one additional hour than the specimens analyzed immediately. The observed fluid advance indicates the possibility that the penetrant oil was lagging behind a "dry" craze "tip" front. A contrasting result was obtained from a similar experiment conducted on samples previously deformed at 1.0 kbar. The results are shown in Fig. 2(B). In this case, slight regression has been observed which may indicate a normal drainage and possible "healing" effects of crazes that have been filled with environmental liquid during deformation. This observation implies that the pressure must have been high enough to cause the oil front to follow the very tip of the growing craze front.

The results shown in Fig. 2 (A) and (B) indicate the decrease of craze size and density as a function of pressure. This can be easily seen by comparing the initial concentration profiles of both cases where samples were similarly deformed for the same period of time but at different pressures: 10 and 1000 bars.

### 3.3. Driving Force of Liquids into Crazes

Although there is general agreement that the kinetics of liquid transport into crazes follows one form or another of Darcy's

law<sup>1, 5, 6</sup>, the question of whether the liquid is driven by atmospheric or capillary pressures remains unsettled.

To elucidate the nature of the driving force of liquids into crazes, a simple experiment was considered. Cylindrical PS samples were caused to be crazed in air under stress relaxation conditions where the samples were maintained at 1% elongation for four hours. The crazed samples were unloaded and immediately soaked in silicone oil for various periods of time after which FTIR analysis was conducted to determine oil penetration. Results of this experiment are shown in Table I where the penetration is expressed directly in absorbance units.

These results indicate that the liquid readily penetrates the air-filled crazes. The depth of penetration reached about 0.8 mm within 30 minutes and remained unchanged for longer soaking times. Since the crazes are assumingly filled with atmospheric air, the liquid must have been driven by a force that exceeds the 1 atm. pressure prevailing in the entire craze channel. This observation refutes the hypothesis made by Williams and coworkers<sup>7</sup> that atmospheric pressure is the driving force affecting penetration of liquids into crazes. In order that this might happen, a close to zero pressure condition must prevail at the craze tip. Obviously, this condition does not exist, as indicated by the present results.

Therefore, it may be concluded that the capillary pressure, as postulated earlier by Kambour<sup>8</sup> and supported by Kramer and Bubeck<sup>6</sup>, ought to be the driving force of environmental liquids into crazes.

If a craze whose tortuous pores are roughly averaged as circular tubes with an effective radius R is immersed in liquid with large free surface, the liquid surface meets the "wall" at a contact angle  $\theta$ . If  $\theta$  is too small, a highly curved liquid surface is developed which causes a large jump in pressure across the liquid-gas interface (capillary pressure). The capillary pressure so developed may be expressed approximately as

$$\Delta p = \frac{2\gamma \cos \theta}{R}$$

where  $\gamma$  is the surface tension of the liquid.

A reasonable estimate for the average pore diameter R from electron micrographs is on the order of 0.1  $\mu$ . The capillary pressure, according to the above equation, developed across the interface by silicone oil ( $\gamma = 21$  dynes/cm, and  $\theta \sim 0$ ) is found to be 42 atm. This value is much higher than that assumed by Marshall and Williams<sup>7</sup>. It is interesting, however, to note that the value of capillary pressure estimated here is in close agreement with that obtained from the model finessed by Kramer and Bubeck<sup>6</sup>.

In the case of liquids which do not wet the wall of the pore,  $\theta \geq \pi/2$ , and no penetration would occur. This has been confirmed in a study of fluid penetration into precrazed high impact polystyrene (HIPS) where water and mercury, because of their high contact angles, were found not to penetrate the precrazed sample<sup>9</sup>.

#### 3.4. Pressure-Induced Transport Transition

Under elevated hydrostatic pressure, the pressure component acting along the craze adds up to the capillary pressure. The depth of oil penetration, therefore, increases with the applied pressure. This is indicated by the strong pressure dependency of  $-\log \kappa$  (Fig. 1). The accelerated flow effected by the pressure appears to reach its maximum at about 80 bars for this particular experiment. Beyond this point and as the pressure increases, the penetration coefficient is observed to decrease substantially through the second stage, i. e., pressure-suppressed transport. The transport transition seems to coincide with the pressure at which the liquid front is forced to the very tip of the craze tip front (Fig. 2). In the second stage (regimes I and II), the pressure component along the craze (in excess of 80 bars) is thought to exert a wedging effect which is opposed by a process of "void" suppression<sup>1</sup>. The rate at which  $-\log \kappa$  decays with pressure undergoes a sudden change at

about 0.5 kbar, a pressure which has been considered to correspond to a solid state transition.

### 3.5. Effective Axial Strain

In this section, the stress-strain relationship associated with the present experiment is analyzed, in an attempt to understand craze formation and growth under triaxial loading conditions. As pointed out earlier, the experiment was conducted in a stress-relaxation mode (fixed nominal elongation). Figure 3 schematically illustrates the response of a two dimensional element (for the sake of simplicity) to a two step loading scheme: hydrostatic pressure then axial deformation.

A hydrostatic pressure  $p_1$  applied to the initial element (represented by a solid line) will cause it to assume its compressed state (dashes). If, on the other hand, another pressure  $p_2 > p_1$  is applied, the element assumes a more compressed state (dots). Subsequently, when a nominally fixed axial elongation  $\epsilon^*$  is applied, the effective axial elongation at  $p_1$  and  $p_2$  would be  $\epsilon_1$  and  $\epsilon_2$  respectively. In general, the effective axial deformation may be expressed as

$$\epsilon = \epsilon^* - \frac{1 - 2\nu}{E(p)} p$$

where  $\nu$  is Poisson's ratio and  $E$  is Young's modulus. For  $\nu = 0.33$  (PS), the stress-strain relationship, under a series of pressures within the range of our experiment, is shown in Table II. The global stress  $\bar{\sigma}$  is obtained from the relation  $\bar{\sigma} = \sigma_{\infty} - p$ , where  $\sigma_{\infty}$  is the applied axial load divided by the cross-sectional area.

Whereas a global negative stress is exerted on the sample at pressures higher than 30 MPa, the analysis shows that the sample still undergoes positive axial (tensile) deformation. This result explains the formation of crazes (dilatational structures) under compressive stress state. Furthermore, the sharp reduction in the effective axial strain estimated for the high pressure end of our experiment may also explain the reduction in craze density and size described earlier.

### 3.6. Effect of Oil Penetration on Craze Growth

At atmospheric pressure, it has been shown that the liquid front lags considerably behind the dry craze tip front<sup>1</sup>. In this report, it is instructive to visualize the effect of penetrant liquid on the craze growth conditions. When samples were held at 1% elongation in air, no failure occurred for more than 10 hours despite intensive crazing. On the other hand, when the same experiment was repeated in silicone oil (500 cS), the sample fractured within about 85 minutes. Although this oil was found to exert a negligible

effect on the craze initiation stress at atmospheric pressure<sup>10, 11</sup>, there appears to be a certain environmental effect in the time scale of the present experiment. For the purpose of understanding this effect, we shall consider the stress distribution within a PS craze recently reported by Kramer<sup>12</sup>. Figure 4 shows the stress distribution within a craze of length  $l_1$  grown in air under a remote average stress  $\sigma_\infty$ . An independent study with crazed HIPS<sup>13</sup> showed that silicone oil (500 cS) can cause an irreversible stress relaxation of about 40% within a time scale comparable to that of the present experiment. Therefore, a shift in the stress equilibrium along the craze is expected and may be approximated by the lower distribution shown in Fig. 4. Of course, the exact distribution will be a function of the exact location of the liquid front and the time history of the craze. However, the relaxed stress equilibrium suggested requires the displacement of the craze tip from  $l_1$  to  $l_2$ . This enhanced craze growth is a time-dependent operation that is closely associated with the capillary pressure and the hydrodynamic permeability (penetrability) of the liquid into the porous craze structure.

As the pressure increases within the first stage (Fig. 1), the liquid front proceeds closer to the tip and the relaxation-induced craze tip advance is enhanced. This simplified approach can not be easily applied to craze growth under higher pressures since other

complicacies are involved including the effect of pressure on stress relaxation, yield stress, "void" suppression and the wedge effect of the pressure component along the craze.

### 3.7. Pressure-Induced Craze Suppression

As the applied pressure was increased during the second stage (regimes I and II), the craze density and size were observed to be reduced drastically. Ultimately, at a pressure slightly above 1.2 kbar, only a few meager crazes appeared on the surface and no measurable penetration was detected. That crazes are thin and short may generally be understood from the magnitude of the effective strain analysis (Table II). To elucidate the possible mechanism by which the pressure causes intensive reduction in the density of crazing we propose the following analysis.

Since crazing is sensitive to surface perfection, it is useful to consider the average distribution of surface heterogeneities along the gauge length of the sample. Fortunately, the average surface roughness of PS samples prepared in a fashion similar to that used in our experiment has been determined by Argon and Hannosh<sup>14</sup>. The distribution of surface grooves of various aspect ratios reproduced from a histogram published in that report is shown in Fig. 5. A distribution similar to that shown in Fig. 5, in which the aspect ratio of the grooves varies over an order of magnitude, is not

uncommon. For the sake of simple illustration, however, we shall consider three hypothetical grooves varying in aspect ratio (Fig. 6). The stress concentration,  $c$ , associated with each groove will be proportional to its aspect ratio, i.e.,  $c_1 > c_2 > c_3$ .

In the case of a liquid-filled groove, the maximum stress at its tip as a function of pressure is given by<sup>15</sup>

$$\sigma_{\max}^f = c_1 \sigma_{\infty} - p$$

where  $\sigma_{\infty}$  is the remote tensile stress and  $p$  is the applied hydrostatic pressure. The relationship  $\sigma_{\max 1} > \sigma_{\max 2} > \sigma_{\max 3}$  would always prevail under any pressure. Furthermore, as the pressure is increased,  $\sigma_{\max}$  will decrease monotonically in a fashion similar to that illustrated in Fig. 7. According to the criterion of craze initiation under pressure presented recently by Baer and coworkers<sup>15</sup>, a craze is initiated when  $\sigma_{\max}$  at the root of a groove reaches a pressure-independent critical stress  $\sigma_c$ .

Due to the relatively large magnitude of  $c_1$  the decreasing maximum stress associated with the first groove ( $\sigma_{\max 1}$ ) will always remain above  $\sigma_c$ . Therefore, craze initiation is permissible at the root of this groove within the entire range of pressure. On the other hand, grooves 2 and 3, due to their relatively smaller stress concentrating effect, would not qualify

for craze initiation at pressures below  $p_{c_2}$  and  $p_{c_3}$ , respectively. This is attributed to the fact that the maximum stresses associated with both grooves at these two pressures fall below  $\sigma_c$ . Therefore, not all surface imperfections are expected to initiate crazes at elevated pressures. In other words, the number of craze-initiating surface heterogeneities would diminish as a function of pressure.

According to this analysis, and to better understand the pressure-induced reduction of craze density, we depict the probability density of crazes at various pressures. Figure 8 illustrates such distributions as a function of  $\sigma_{max}$  at three pressures:  $p_3 > p_2 > p_1$ . For a fixed  $\sigma$ , it is obvious that the density of crazes occurring under  $p_3$  is but a small fraction of that which may occur at  $p_1$ . This illustration provides a clear explanation of the extensive reduction in craze density observed in the range of 0.5 to 1.2 kbar.

4. SUMMARY AND CONCLUSIONS

The penetration coefficient of silicone oil into PS, axially deformed in tension under superposed hydrostatic pressure, increases dramatically with pressure (first stage) then decreases through a second stage in two regimes. In the first stage, the lagging fluid front is forced towards the "dry" craze tip front. A transport transition occurs when a "void" suppression effect reaches a magnitude comparable to the pumping pressure. The transport suppression observed in the second stage is accompanied by reduction in craze density and size where the change in transport behavior from regimes I to II is possibly related to a (glass-glass) solid state transition.

At atmospheric conditions, an estimated capillary pressure on the order of  $4\text{MNm}^{-2}$  drives the low surface tension liquid against its hydrodynamic permeability. Craze tip advance is proposed to result from the shifting of equilibrium stress within the craze due to the induced stress relaxation in the mature part of the craze.

An effective axial strain analysis shows that a small, but positive, tensile strain is effected even at pressures where the macroscopic stress state is compressive.

Based on the maximum stress criterion for craze initiation, in association with experimentally determined surface roughness distribution, a mechanism is proposed to explain the pressure-induced suppression of the number of crazes.

ACKNOWLEDGEMENTS

The authors gratefully acknowledge the financial support of this work by the Office of Naval Research through Contract Number N00014-75-C-0795. We are most thankful to Professor I. Palley for his helpful comments.

REFERENCES

1. A. Moet and E. Baer, J. Mater. Sci., 15 (1980) 31.
2. R. Narayan Swamy, Ibid, 14 (1979) 1521.
3. A. Moet, I. Palley and E. Baer, VI Inter-American Conference on Materials Technology, San Francisco, California (1980).
4. H. Ll. Pugh, (Ed), High Pressure Engineering, Mechanical Engineering Publications Ltd, London (1975) p. 41.
5. G. P. Marshall, L. E. Culver and J. G. Williams, Proc. R. Soc. London A, 319 (1970) 165.
6. E. Kramer and R. A. Bubeck, J. Polym. Sci:Phys. Ed., 16 (1978) 1195.
7. J. G. Williams and G. P. Marshall, Proc. R. Soc. London, A, 342 (1975) 55.
8. R. P. Kambour, J. Polym. Sci. Macromol. Rev., 7 (1973) 1.
9. A. Moet, I. Palley and E. Baer, J. Appl. Phys, in press.
10. R. P. Kambour, C. L. Gruner and E. E. Romagosa, J. Polym. Sci., A-2, 10 (1973) 1789.
11. K. Matsushige, S. Radcliff and E. Baer, J. Mater. Sci., 10, (1975) 833.
12. E. J. Kramer, B. D. Lauterwasser, Fourth Internal Conference on Deformation, Yield and Fracture of Polymers, Cambridge, U. K. (1979).
13. K. Walton, A. Moet and E. Baer, to be published.
14. A. S. Argon, J. G. Hannoosh, Philos. Mag., 36 (1977) 1195.
15. A. Moet, I. Palley and E. Baer, ACS meeting "Organic Coatings and Plastics Chemistry", vol. 41, (1979) 424.

TABLE I: Free penetration of silicone oil (500 cS) into precracked samples for various soaking times. Samples are crazed for 4 hrs at 1% elongation in air.

Depth (m x 10 <sup>4</sup> )	1.3	2.5	3.8	5.1	7.6	8.9	10.2
15 minutes	0.45	0.11	0	0	-	-	-
30 minutes	0.76	0.34	0.23	0.21	0.06	0	-
90 minutes	0.71	0.33	0.24	0.18	0.09	0	-

TABLE II: The effective axial strain and the associated stress calculated at 1% fixed elongation as a function of pressure.

Applied pressure (MPa)	0.1	20	40	60	80	100
Global stress (MPa)	31.1	11.2	-7.8	-27.4	-46.5	-64.2
Maximum stress (MPa)	93	73	56	37	20	7
Effective axial strain (%)	1.0	0.8	0.6	0.4	0.2	0.05

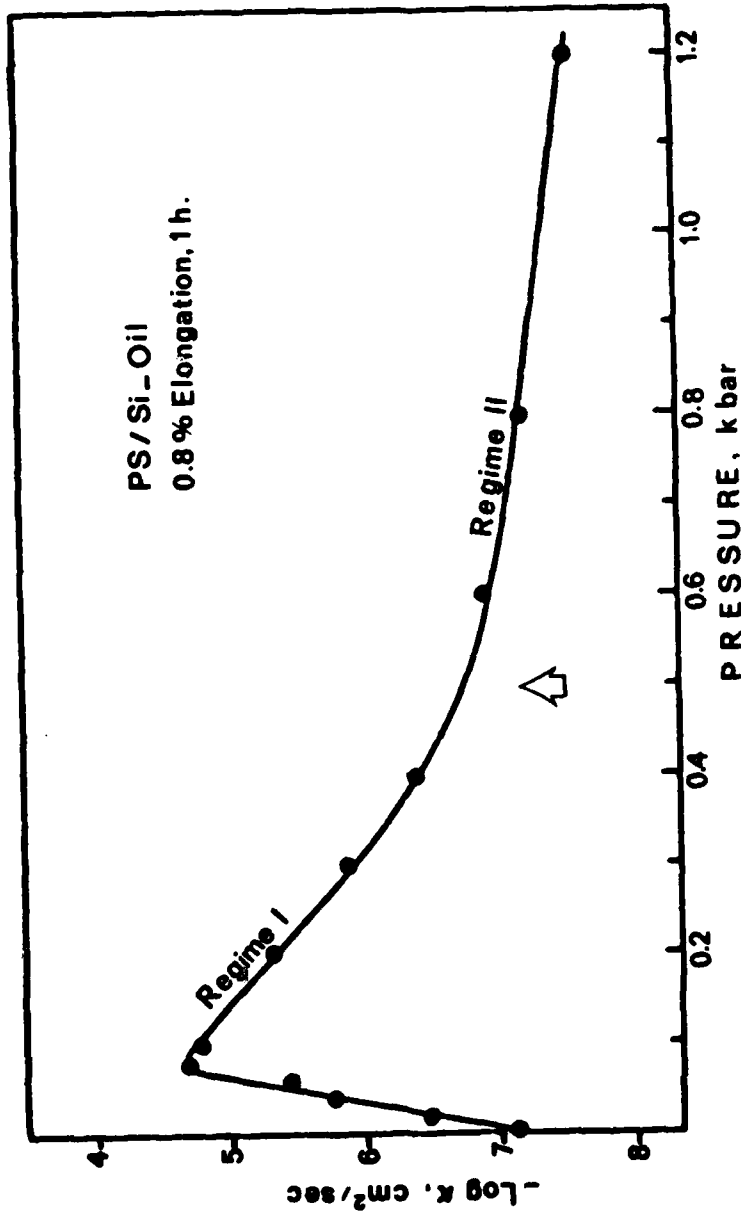


Fig. 1. Dependency of the penetration coefficient ( $-\log \kappa$ ) of silicone oil (500 cS) into PS elongated to 0.8% for 1 h. The arrow indicates a solid state-transition.

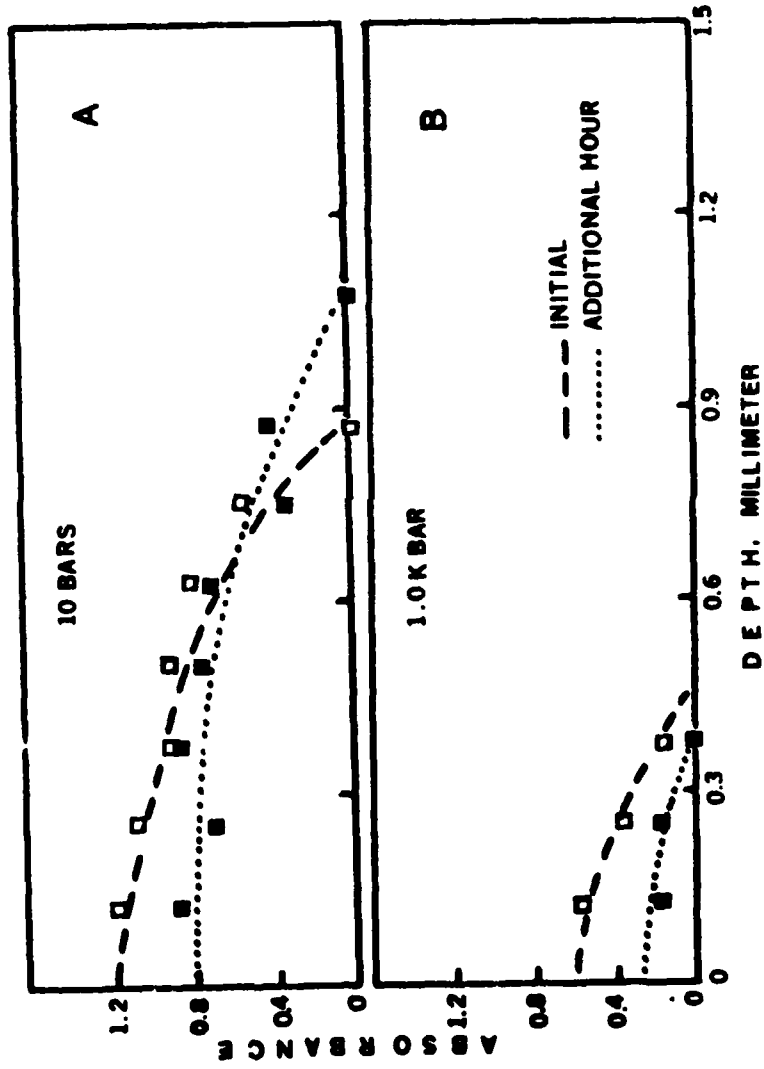


Fig. 2. The effect of additional unloaded soaking for 1 h of PS initially deformed to 0.8% elongation in silicone oil at 10 bars (A) and 1 kbar (B).

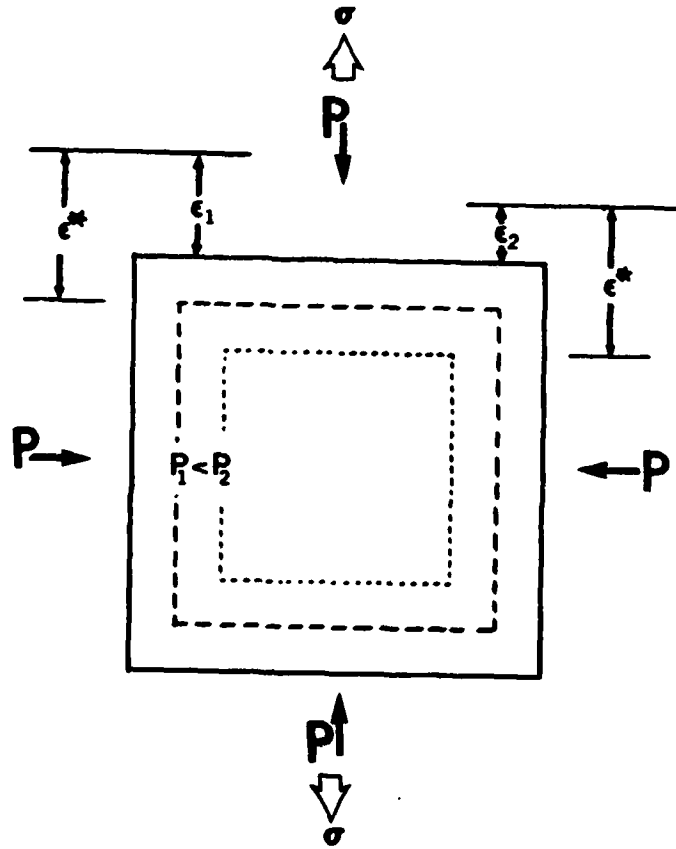


Fig. 3. Schematic of the effective axial strain for a two dimensional element elongated under superposed hydrostatic pressure. A constant applied elongation  $\epsilon^*$  results in effective axial strains of  $\epsilon_1 > \epsilon_2$  at pressures of  $p_1 < p_2$ , respectively.

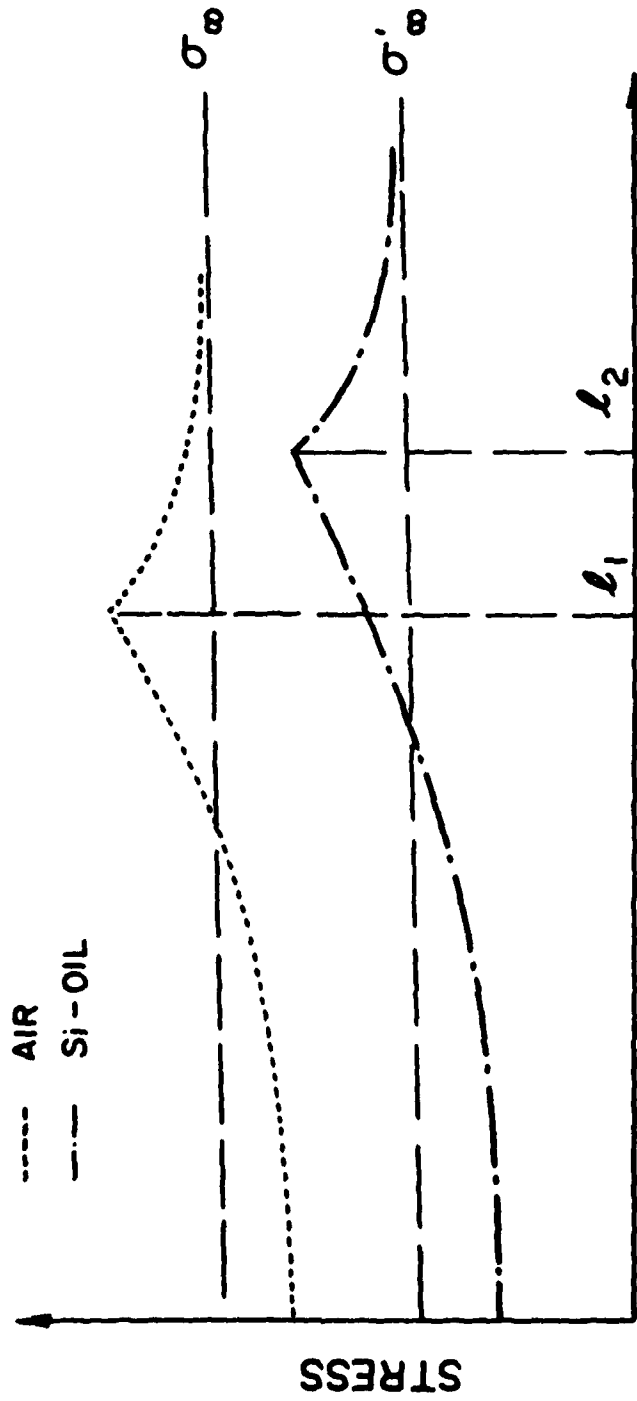


Fig. 4. A schematic representing the stress redistribution along a partially silicone oil-filled craze (lower curve) with respect to that of a dry craze (upper curve). Note that a drop of the remote stress from  $\sigma_0$  to  $\sigma'_0$  causes a craze tip advance from  $l_1$  to  $l_2$ .

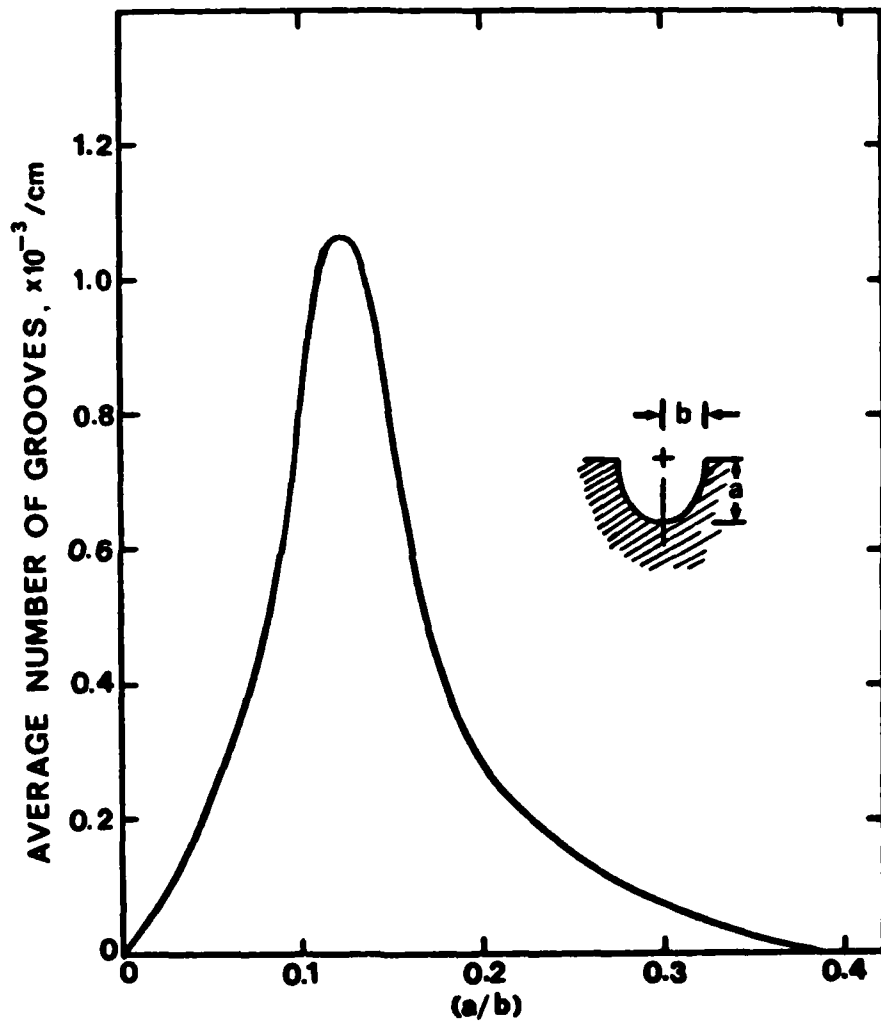


Fig. 5. The distribution of surface grooves of various aspect ratios (a/b) determined experimentally for PS samples treated in a fashion similar to our samples<sup>14</sup>.

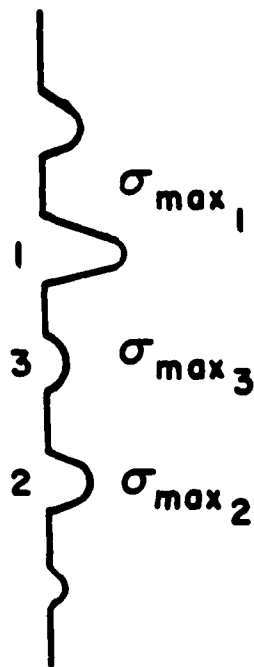


Fig. 6. A schematic representation of three surface grooves associated with  $\sigma_{max_1} > \sigma_{max_2} > \sigma_{max_3}$ , to be considered for deformation under pressure.

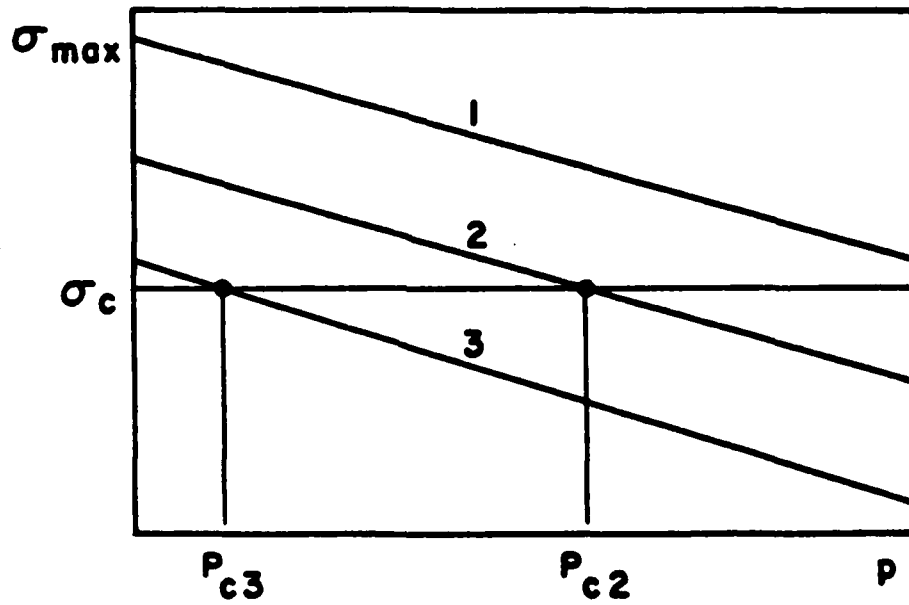


Fig. 7. The effect of pressure on the maximum stress associated with the three hypothetical grooves illustrated in Fig. 6 in conjunction with the critical craze initiation stress  $\sigma_c$ .

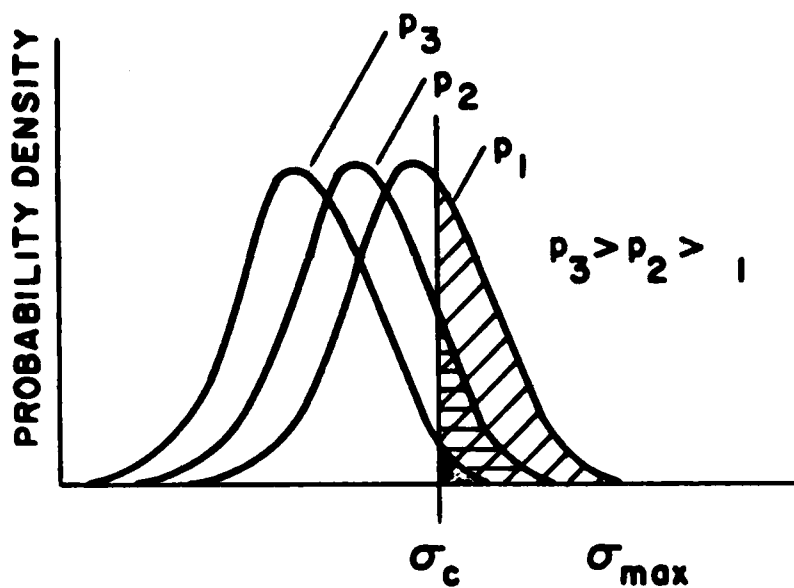


Fig. 8. A schematic of the effect of pressure on the distribution of the stress-raising capacity of surface grooves. The shaded area under each curve represents the possible number of craze sites at the corresponding pressure.